



## Flexible Thermoelectric Thin Film Devices

Chatchavit Seetawan<sup>1</sup>, Atiwat Seetawan<sup>2</sup>, Chutpong Paiyasan<sup>2</sup>, Phanomphan Chaiyapet<sup>1,2</sup>, Somporn Thaowankaew<sup>3</sup>, Pennapa Muthitamongkol<sup>4</sup>, Urai Seetawan<sup>1,\*</sup>

<sup>1</sup>Enrichment Program of Science Mathematics Technology and Environment, Thatnaraiwittaya School, 606 Nittayo Road, That Choeng Chum, Mueang Sakon Nakhon, Sakon Nakhon, 47000 Thailand

<sup>2</sup>English Program, Thatnaraiwittaya School, 606 Nittayo Road, That Choeng Chum, Mueang Sakon Nakhon, Sakon Nakhon, 47000 Thailand

<sup>3</sup>Thin Film Research Laboratory, Center of Excellence on Alternative Energy, Research and Development Institute, Sakon Nakhon Rajabhat University, 680 Nittayo Road, That Choeng Chum, Mueang Sakon Nakhon, Sakon Nakhon, 47000 Thailand

<sup>4</sup>Microscopy and Microanalysis Section, National Metal and Materials Technology Center, 114 Thailand Science Park, Phaholyothin Road, Klong 1, Klongluang, Pathumthani, 12120 Thailand

\*Corresponding Author: [useetawan@yahoo.com](mailto:useetawan@yahoo.com)

Received: 14 November 2019; Revised: 6 January 2020; Accepted: 14 January 2020; Available online: 1 May 2020

## Abstract

Flexible thermoelectric devices (F-TEDs) thin film has been converted heat from chest skin energy to electrical energy. We proposed the novel uni-leg TEDs thin film using a polyimide (PIM) flexible substrate as low thermal conductivity and minimize heat losses, n-Bi<sub>2</sub>Te<sub>3</sub> thermoelement very good properties at low temperature and Ag electrode thin films as non-oxidization fabricated by DC magnetron sputtering method and annealed this film at 473 K for 8 min. The F-TEG thin film placed on chest skin has been generated maximum output electrical voltage 8.90 mV and electrical power 1.20  $\mu$ W cm<sup>-2</sup> at different temperature between the chest skin and ambient air about 5 – 7 K.

**Keywords:** Nano and micro generator; Flexible thermoelectric generator; Harvesting energy; Electricity from human body heat; Thermoelectric thin film

©2020 Sakon Nakhon Rajabhat University reserved

## 1. Introduction

In the future, the harvesting energy storage for using in the 21<sup>st</sup> century with artificial intelligence (AI) such as flexible wearable electronic devices, stretchable human-interactive sensors, displays and the thermoelectric devices (TEDs) [1, 2]. TEDs can convert waste heat into the electricity about 2,500 mW cm<sup>-2</sup> and apply the electrical power directly into a cooler and heater [3 – 5]. The commercial thermoelectric materials have an n-type bismuth telluride (Bi<sub>2</sub>Te<sub>3</sub>) and p-type antimony telluride (Sb<sub>2</sub>Te<sub>3</sub>) show the thermoelectric figures of merit ( $ZT = S^2 \sigma T / \kappa$ ) about 0.84 and 0.50 at 300 K, respectively and the power factors of  $4.87 \times 10^{-3}$  W m<sup>-1</sup> K<sup>-2</sup> and  $2.81 \times 10^{-3}$  W m<sup>-1</sup> K<sup>-2</sup> at 300 K, respectively [5, 6]. Recently, the wearable electronic devices of TEDs can generate an electricity about 7.40 W cm<sup>-3</sup> [7, 8]. However, the TEDs show inflexible bring anything very difficult to apply with human body skin [9]. On the other hand, the F-TEDs have many applications for example body-powered devices, self-powered wearable health, environmental sensor and wearable energy harvesting [10 – 12]. The F-TEDs have converted a heat from human body skin into the electrical power about 2.10 nW at different temperature between human body skin and ambient air at  $\Delta T = 19$  K [13 – 16] and 4.78 mW cm<sup>-2</sup> and 20.80 mW g<sup>-1</sup> at  $\Delta T = 25$  K [17]. Otherwise, the TEDs are placed on the human body skin heat,

$T_b = 310$  K and ambient air,  $T_a = 295$  K show very low quality thermal coupling and temperature gradient, hence a low electricity [18]. Nevertheless, the thin TEDs are generated electricity from body skin heat with ambient air about  $28.50 \mu\text{W cm}^{-2}$  an efficiency increasing 30% [19] and apply  $20 \mu\text{W}$  to the continuously wearable electronic sensors with no air flow [20 – 21]. The  $\pi$ -type of F-TEGs are fabricated from the n- $\text{Bi}_2\text{Te}_3$  thermoelements of 24 pairs with Ag electrode to generate the output electrical power  $1 – 4 \mu\text{W cm}^{-2}$  at  $\Delta T = 2 – 4$  K [22]. Previously studies, the F-TEDs are p-n junction or  $\pi$ -type used many p and n types thermoelectric materials which do not save cost and difficult to paste on human body skin.

In this study, we present novel fabrication of F-TEDs (uni-leg n- $\text{Bi}_2\text{Te}_3$  thermoelement thin film) for optimizing difficult placed on human body skin deposited on polyimide flexible substrates which low thermal conductivity of PIM ( $0.16 \text{ W m}^{-1} \text{ K}^{-1}$ ) by the DC magnetron sputtering method. The thermoelectric properties of n- $\text{Bi}_2\text{Te}_3$  thermoelement thin film are investigated. In addition, the relationship of electrical voltage output and electrical power output with an electrical resistance of F-TEDs thin film placed on chest skin heat with ambient air at  $\Delta T = 5 – 7$  K are evaluated.

## 2. Materials and Methods

F-TEDs thin film were deposited on polyimide substrates by DC magnetron using  $\text{Bi}_2\text{Te}_3$  target of 99.99% purity for 76.20 mm diameter and 3.00 mm thickness. The mask and electrode of thermoelectric thin film are designed size width 50 mm and length 60 mm for 2 parallel parts, each part compose of 25 legs width 1 mm and long 24 mm, the cell gap about 0.50 mm, PIM  $50 \times 60 \text{ mm}^2$  with supporting maximum temperature of + 673 K and substrate holder rotation about 40 rpm. In DC magnetron sputtering method, the thin n- $\text{Bi}_2\text{Te}_3$  thermoelement on PIM were deposited base pressure  $3 \times 10^{-5}$  Torr for high vacuum, Ar flow rate of 30 sccm for 30 min before sputtering process and the thin Ag thermoelement used pressure  $1.70 \times 10^{-2}$  Torr, electrical current 100 mA and electrical voltage 630 V sputtering for 1 min in Ar gas. And then, the thin n- $\text{Bi}_2\text{Te}_3$  thermoelement and Ag electrode annealed by furnace tube vacuum using pressure  $5.00 \times 10^{-2}$  Torr at 200 °C under high vacuum furnace (Mila5000, Advance) for 8 min in Ar gas to obtain the F-TEDs thin film. In laboratory scale, we fabricated the flexible thin film uni-leg module within 11 pairs on PIM substrate size  $25.40 \times 25.40 \text{ mm}^2$  area and used Ag to make electrode series between TE elements are shown in Fig. 1 (a). The F-TEDs thin film connected with Cu wide for measuring electrical voltage output and application by placed on human skin hot and ambient air cool side for generate electrical power are shown in Fig. 1(b). Phase identification of TE thin films was analyzed by X-ray diffractometer (XRD, XRD6100, Shimadzu) with a Cu source ( $\lambda = 1.54 \text{ \AA}$ ) as used 40 kV and 40 mA in conventional  $2\theta$  mode from  $30^\circ – 50^\circ$  at a step size of  $0.02^\circ$  and a scanning rate of  $8^\circ/\text{min}$ . The microstructure of F-TEDs thin film was observed by Transmission Electron Microscope (TEM; TEM2100 Plus, JEOL), Scanning Electron Microscope (SEM; JSM 7800F Prime, JEOL) and evaluated the chemical composition by Energy Dispersive X-ray Spectrometer (EDS; JSM 7800F Prime, JEOL). The electrical resistivity and Seebeck coefficient were measured by the Seebeck Coefficient / Electric Resistance Measurement System ZEM 3 series (ZEM-3; Advance Riko) at temperature range 310 – 380 K. Moreover, we determinates the power factor from the relationship  $PF = \frac{S^2}{\rho}$  at the same temperature range using different temperature between TEDs thin film and PIM.

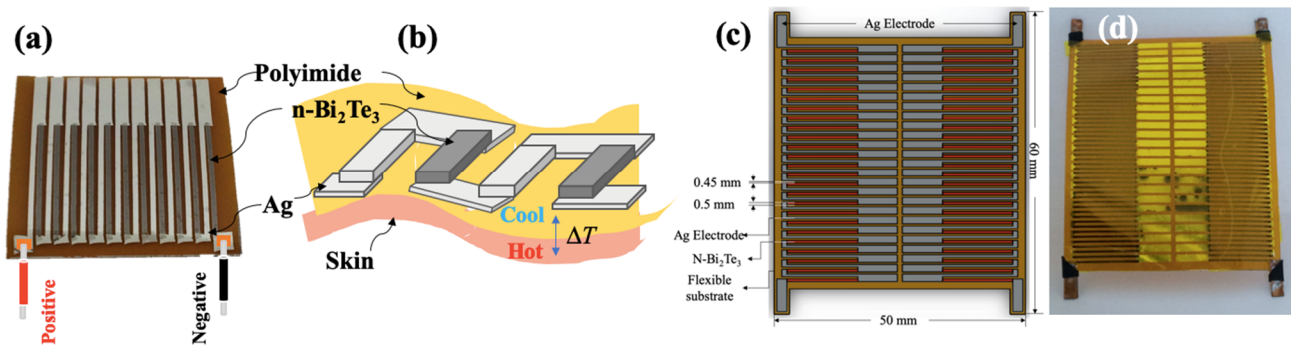


**Fig. 1** (a) Flexible thermoelectric thin film unileg-Bi<sub>2</sub>Te<sub>3</sub> for laboratory scale and (b) Cross-section view of F-TEDs thin film, (c) design F-TEDs thin film on flexible substrate and (d) F-TEDs thin film on polyimide substrate.

The F-TEDs thin film are easily application on chest skin and possibly connected with any micro electronic devices. The relationship between different temperature range 0 – 40 K and open circuit electrical voltage of 50 legs are shown in Fig. 1(c) and Fig. 1(d), respectively. The thermometer, multimeter, heater and F-TEDs thin film are setup for measure electricity.

The electrical power generation of F-TEDs thin film was investigated by evaluating the open voltage ( $V_o$ ) from the 6 ½ digits digital multi-meter (M3500A, Picotest) as related the different temperature ( $\Delta T$ ). At  $\Delta T$  of  $V_o$  highest, the  $\Delta T$  is soaked to measure the electrical current ( $I$ ) with the Picoammeter (648 picometers, Keithley) and output voltage within the various loads apply until 10 M $\Omega$  for calculating the electrical power ( $P = IV$ ) to obtain the maximum power ( $P_{max}$ ).

### 3. Results and Discussion

#### *Crystal Structure*

The XRD spectrum of Bi<sub>2</sub>Te<sub>3</sub> thin film showed a growth along the (0110) plane of Bi<sub>2</sub>Te<sub>3</sub> crystal confirming with JCPDF # 00-008-0021, as shown in Fig. 2.

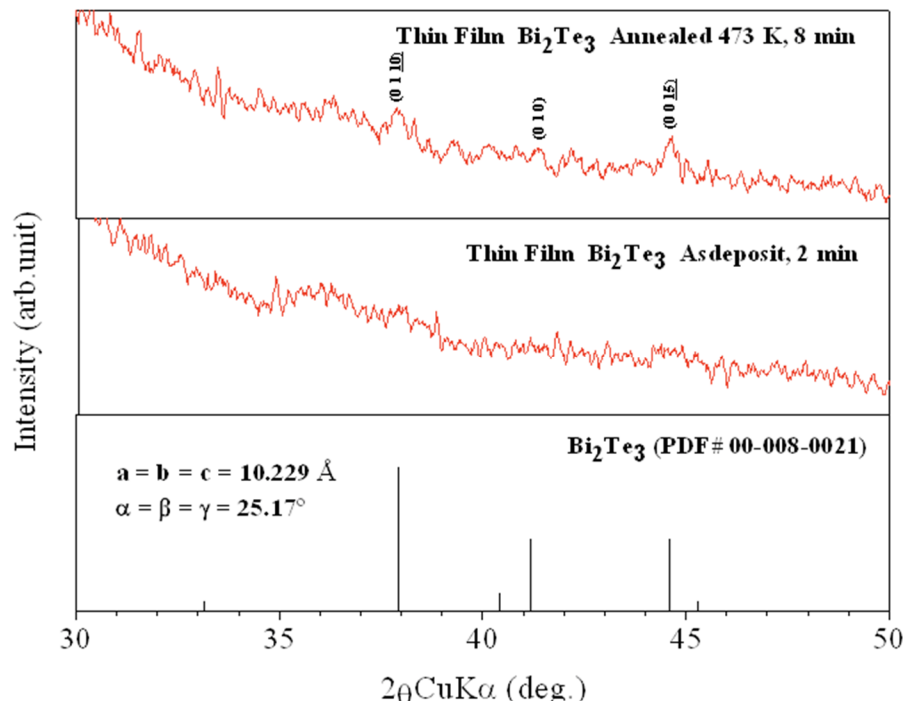


**Fig. 2** XRD of  $\text{Bi}_2\text{Te}_3$  (a) JCPDF # 00-008-0021, (b) target and (c) thin film.

The thin film as a deposit shows a similarly amorphous phase but it's good conduction. So that, we improved the amorphous phase to crystal phase by annealed the thin film at 473 K for 8 mins to obtain (0110), (010) and (0015) planes [23]. The thickness thin film shows very thin order microscale and chemical composition little shift from  $\text{Bi} : \text{Te} ; 2 : 3$  which we discuss and confirm from SEM, EDS and TEM results.

#### Nanostructure

The morphology of F-TEDs thin film of  $\text{Bi}_2\text{Te}_3$  was evaluated by SEM and TEM to obtain the particle size about 16.96 nm, as shown in Fig. 3.

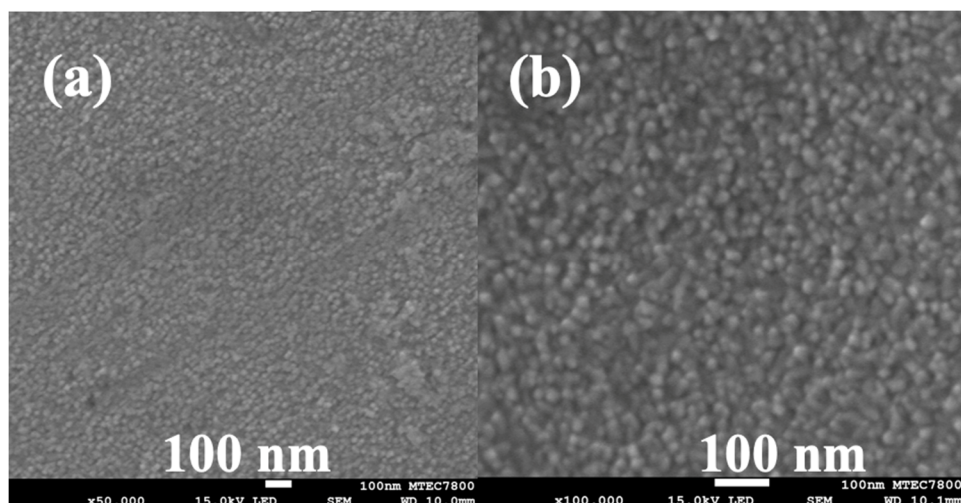


**Fig. 3** SEM images (a)  $\text{Bi}_2\text{Te}_3$  thin films  $\times 50,000$  and (b)  $\text{Bi}_2\text{Te}_3$  thin films  $\times 100,000$ , respectively.

The SEM image of  $\text{Bi}_2\text{Te}_3$ , nanostructure and chemical compositional of  $\text{Bi}_2\text{Te}_3$  were analyzed by TEM and EDS compositional maps of Bi, as shown in Fig. 4(c) and Te elements is shown in Fig. 4(d) corresponding Fig. 4(b), respectively. Which, Bright-field images  $\text{Bi}_2\text{Te}_3$  nanoparticles are Focused Ion Beam (FIB) milling [24], as shown in Fig. 4(a). The film thickness was evaluated by SEM and TEM images around 100 – 150 nm.

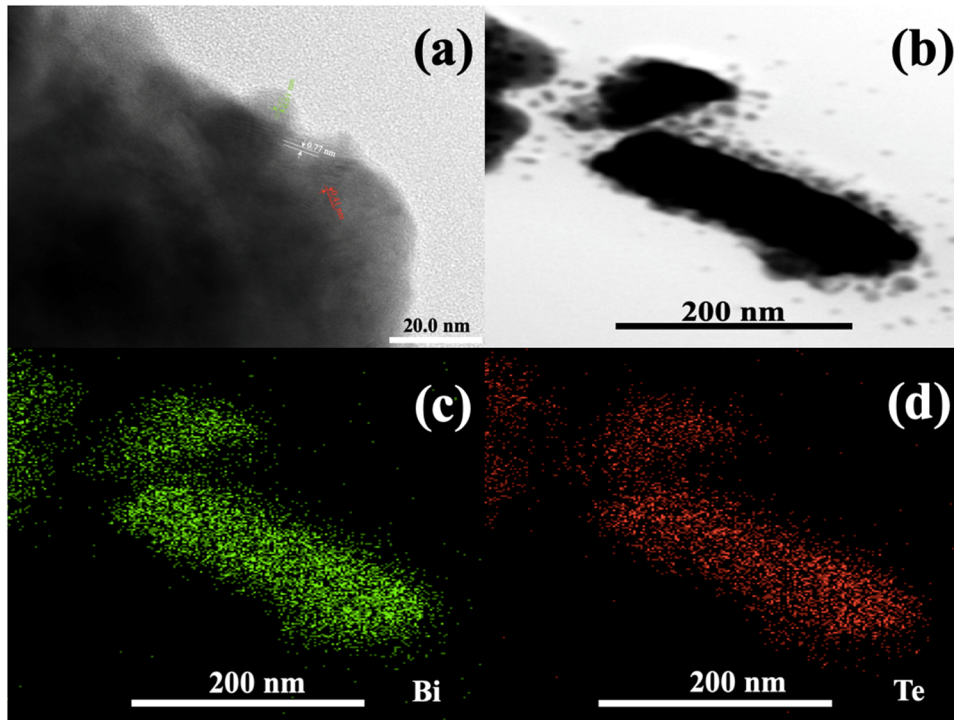


**Fig. 4** (a) TEM image of  $\text{Bi}_2\text{Te}_3$ , (b) SEM image of  $\text{Bi}_2\text{Te}_3$ , (c) and (d) Microstructural and compositional analysis of  $\text{Bi}_2\text{Te}_3$  by EDS compositional maps of Bi, and Te elements, respectively, corresponding to (b).

#### *Thermoelectric Properties*

The temperature dependent on resistivity, Seebeck coefficient and power factor are shown in Fig. 5 as tempearture has showed the power factor value was lower than literature [6]

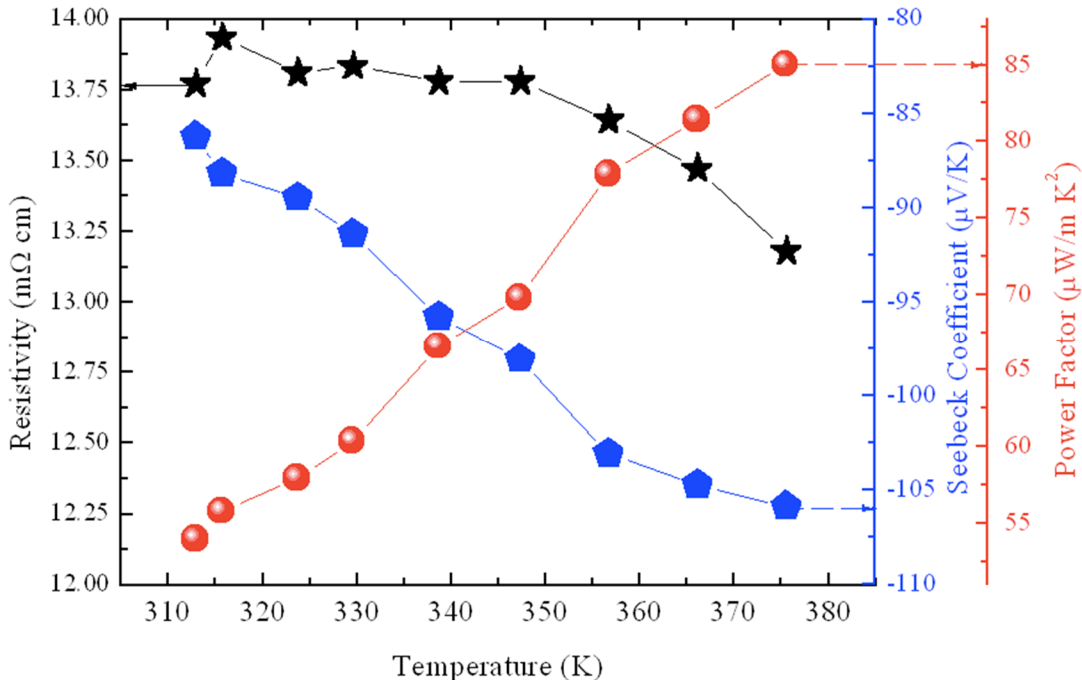


**Fig. 5** The resistivity, Seebeck coefficient and power factor versus temperature for Bi<sub>2</sub>Te<sub>3</sub> thermoelectric thin film.

Because the thin film similar amorphous phase from XRD result and very thin order mircoscale from SEM and TEM results. These parameters can be discussed as following by

$$S_{n,Ag} = -\frac{\Delta V}{\Delta T} \quad (1)$$

$$\rho_{n,Ag} = \frac{R_n + R_{Ag}}{l_{n,Ag} A} \quad (2)$$

$$PF = \frac{S_{n,Ag}^2}{\rho_{n,Ag}} \quad (3)$$

where  $\Delta V$  is different voltage (V),  $\Delta T$  is different temperature (K),  $\rho_n$  is electrical resistivity of Bi<sub>2</sub>Te<sub>3</sub> ( $\Omega$  m),  $\rho_{Ag}$  is electrical resistivity of Ag ( $\Omega$  m),  $l_n$  is length of Bi<sub>2</sub>Te<sub>3</sub> (m),  $l_{Ag}$  is length of Ag (m),  $R_n$  is electrical resistance of Bi<sub>2</sub>Te<sub>3</sub> ( $\Omega$ ),  $R_{Ag}$  is electrical resistance of Ag ( $\Omega$ ),  $S_n$  is Seebeck coefficient of Bi<sub>2</sub>Te<sub>3</sub> ( $V K^{-1}$ ),  $S_{Ag}$  is Seebeck coefficient of Ag ( $V K^{-1}$ ), and  $PF$  is power factor of Bi<sub>2</sub>Te<sub>3</sub> ( $W m^{-1} K^{-2}$ ).

#### *Electrical Resistance, Voltage, and Power Output*

The electrical voltage output, electrical power output versus electrical resistance for F-TEDs thin film of 50 pairs were obtained maximum value about 17 mV and 2.50 nW at  $\Delta T = 40$  K [9 – 12], as shown in Fig. 6.

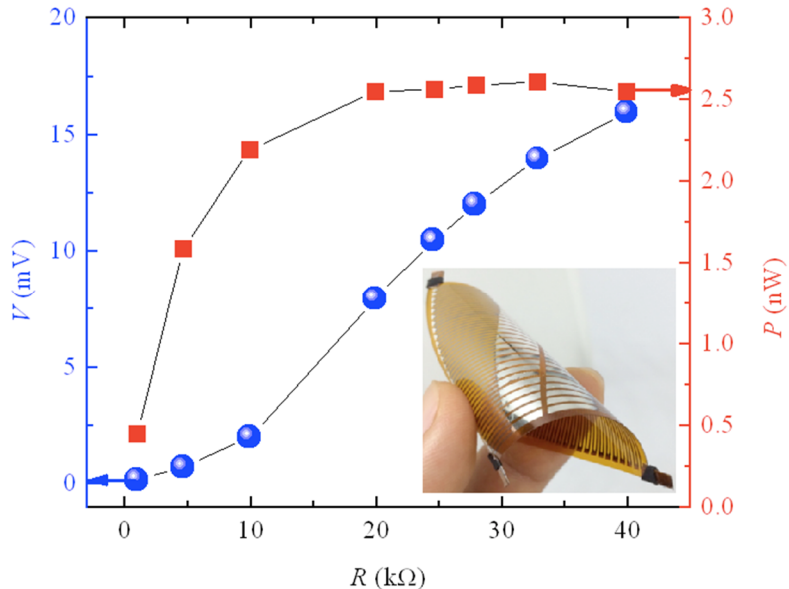


**Fig. 6** The electrical voltage output, electrical power output versus electrical resistance for  $\text{Bi}_2\text{Te}_3$  thermoelectric thin film.

The electrical voltage and electrical power were increased with increasing resistance load agreement with values reported in the literature [7 – 11]. However, electrical power is depended on matching electrical resistance following by

$$P = I^2 R_L = \left( \frac{(S_n - S_{Ag})(T_h - T_c)}{R_{Ag} + R_n + R_L} \right)^2 R_L \quad (4)$$

$$I = \frac{(S_n - S_{Ag})(T_h - T_c)}{R_{Ag} + R_n + R_L} \quad (5)$$

where  $P$  is electrical power (W),  $I$  is electrical current (A),  $R_L$  is electrical resistance load ( $\Omega$ ),  $T_h$  is temperature hot side (K) and  $T_c$  is temperature cold side (K).

#### F-TEDs Application

We designed F-TEDs thin film for application with chest skin heat source and reduced heat by ambient air to make different temperatures and measuring voltage out put is shown in Fig. 7(a). Moreover, we measured thermal radiation at human body skin for checking different temperature by thermal camara, as shown in Fig. 7(b). We found the maximum body temperature at 307 K and maximum  $\Delta T = 12$  K correspond with Lossec M *et al.* [18]. Therefore, we up size of F-TEDs thin film about  $203.20 \times 203.20 \text{ mm}^2$  compose of uni-leg  $\text{Bi}_2\text{Te}_3$  size width 2 mm and length 50 mm, cell gap about 1 mm used 25 pairs sereis 2 parts totally 50 pairs and placed on chest for area measured electrical voltage and power output about 8.90 mV and  $1.20 \mu\text{W cm}^{-2}$  agreement with reported in the literature [13 – 18], respectively at  $\Delta T = 5 - 7$  K are shown in Fig. 7(c). However, the power factor value shows comparatively lower than the reported value  $4.87 \times 10^{-3} \text{ W cm}^{-2}$ . According to paper, they achieved output voltage and power output having 50 pairs about 17 mV and 2.5 nW, respectively [6]. We designed the  $\Delta T$  of F-TEDs thin film in-plane which it very low value and then we changed their cross-plane to increase  $\Delta T$  from chest skin with ambient air.

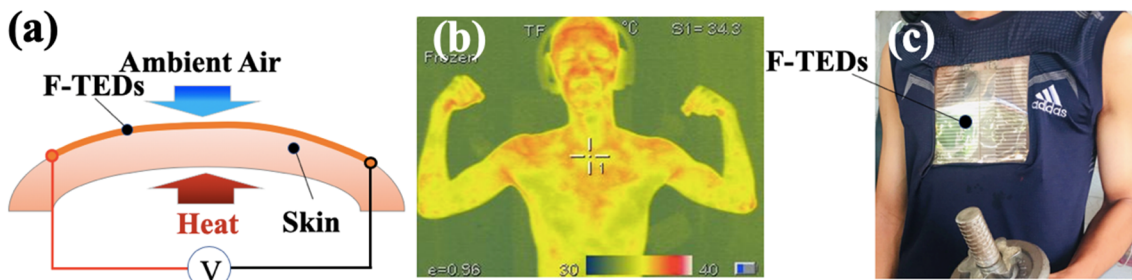


**Fig. 7** Application of F-TEDs (a) diagram placed on human body skin and measuring voltage output (b) measure different temperature radiation at human body skin and (c) placed on chest skin heat.

## 4. Conclusion

The F-TEDs thin film including uni-leg n-Bi<sub>2</sub>Te<sub>3</sub> thermoelectric thin film, Ag electrodes on polyimide substrate and Cu conductor wire for measuring electrical quantity. This study found that the F-TEDs thin film can be generated milli electrical volt and nano to micro electrical watt by placed on chest skin heat side with ambient air cold side get a  $\Delta T = 5 - 7$  K. The F-TEDs thin film were optimized by increasing numbers of cells, different temperature and reducing thermal conductivity of PIM. Suggestion, the improved F-TEDs thin film need to p-n junction which is very important for increasing electrical power output.

## 5. Acknowledgements

This work was financially supported by Thai Thermoelectric Society (TTS) and Research Development Institute (RDI), Sakon Nakhon Rajabhat University.

## 6. References

- [1] M. Gao, L. Li, Y. Song, Inkjet printing wearable electronic devices, *J. Mater. Chem. C.* 5 (2017) 2971 – 2993.
- [2] A. Dewan, U.A. Suat, M.N. Karim, H. Beyenal, Alternative power sources for remote sensors: A review, *J. Power Sources.* 245 (2014) 129 – 143.
- [3] E.B. Lon, Cooling, Heating, Generating Power, and Recovering Waste Heat with Thermoelectric Systems, *Sci.* 31 (2008) 1457 – 1460.
- [4] F.J. DiSalvo, Thermoelectric Cooling and Power Generation, *Sci.* 285 (1999) 703 – 706.
- [5] K.V. Selvan, M.S.M. Ali, Micro-scale energy harvesting devices: Review of methodological performances in the last decade, *Renew. Sust. Energ. Rev.* 54 (2016) 1035 – 1074.
- [6] J.P. Carmo, L.M. Gonçalves, J.H. Correia, Thermoelectric Microconverter for Energy Harvesting Systems, *IEEE T. Ind. Electron.* 57 (2010) 861 – 867.
- [7] M. Lossec, B. Multon, H.B. Ahmed, Sizing optimization of a thermoelectric generator set with heatsink for harvesting human body heat, *Energ. Convers. and Manage.* 68 (2013) 260 – 265.
- [8] M. Wahbah, M. Alhawari, B. Mohammad, H. Saleh, M. Ismail, Characterization of Human Body-Based Thermal and Vibration Energy Harvesting for Wearable Devices, *IEEE J. Em. Sel. Top. C.* 4 (2014) 354 – 363.
- [9] Y. Qi, C. McAlpine, Nanotechnology-enabled flexible and biocompatible energy harvesting, *Energy Environ. Sci.* 3 (2010) 1275 – 1285.
- [10] V. Misra, A. Bozkurt, B. Calhoun, T. Jackson, J.S. Jur, J. Lach, B. Lee, J. Muth, O. O’mer, M. O’zturk, S. Trolier-McKinstry, D. Vashaee, D. Wentzloff, Y. Zhu, Flexible Technologies for Self-Powered Wearable Health and Environmental Sensing, *Proc. IEEE.* 3 (2015) 665 – 681.

- [11] V. Leonov, R.J.M. Vullers, Wearable Thermoelectric Generators for Body-Powered Devices, *J. Electron. Mater.* 38 (2009) 1491 – 1498.
- [12] J. H. Bahk, H. Fang, K. Yazawa, A. Shakouria, Flexible thermoelectric materials and device optimization for wearable energy harvesting, *J. Mater. Chem. C.* 3 (2015) 10362 – 10374.
- [13] I. Stark, Thermal Energy Harvesting with Thermo Life, International Workshop on Wearable and Implantable Body Sensor Networks, Cambridge. 3 – 5 April 2006, 19 – 22.
- [14] S.E. Jo, M.K. Kim, M.S. Kim, Y.J. Kim, Flexible thermoelectric generator for human body heat energy harvesting, *Electron. Lett.* 48 (2012) 1015 – 1016.
- [15] Y. Du, J. Xu, B. Paul, P. Eklund, Flexible thermoelectric materials and devices, *Appl. Mater. Today.* 12 (2018) 366 – 388.
- [16] S.J. Kim, W.J. Hyung, B.J. Cho, Wearable Thermoelectric Generator Fabricated on Glass Fabric, *Energ. & Environ. Sci.* 7 (2014) 1959 – 1967.
- [17] S.J. Kim, H.E. Lee, H. Choi, Y. Kim, J.H. We, J.S. Shin, K.J. Lee, B.J. Cho, High-Performance Flexible Thermoelectric Power Generator Using Laser Multiscanning Lift-Off Process, *ACS Nano* 10 (2016) 10851 – 10857.
- [18] M. Lossec, B. Multon, H.B. Ahmed, C. Goupil, Thermoelectric generator placed on the human body: system modeling and energy conversion improvements, *Eur. Phys. J. Appl. Phys.* 52 (2010) 11103 – 11113.
- [19] T. Krishna, L.H Seittaluri, J.R. Rajeev, Thin Thermoelectric Generator System for Body Energy Harvesting, *J. Electron. Mater.* 41 (2012) 984 – 988.
- [20] F. Suarez, A. Nozariasbmarz, D. Vashaee, C. M. Öztürk, Designing Thermoelectric Generators for Self- Powered Wearable Electronics, *Energ. Environ. Sci.* 6 (2016) 1853 – 1890.
- [21] S. Qing, A. Rezania, L.A. Rosendahl, X. Gou, Design of flexible thermoelectric generator as human body sensor, *Proc. Mater. Today.* 5 (2018) 10338 – 10346.
- [22] N.H. Trung, N.V. Toan, T. Ono, Fabrication of type flexible thermoelectric generators using an electrochemical deposition method for thermal energy harvesting applications at room temperature, *J. Micromech. and Microeng.* 27 (2017) 125006.
- [23] E. Vieira, J. Figueira, A.L. Pires, J. Grilo, M.F. Silra, A.M. Pereira, L.M. Goncalves,  $\text{Bi}_2\text{Te}_3$  and  $\text{Sb}_2\text{Te}_3$  Thin Films with Enhanced Thermoelectric Properties for Flexible Thermal Sensors, *Eurosensors 2018*, Graz, Austria. 9 – 12 September 2018, 815 – 819.
- [24] J. Mayer, L.A. Giannuzzi, T. Kamino, J. Michael, TEM Sample Preparation and FIB-Induced Damage, *MRS. Bull.* 32 (2007) 400 – 407.